Journal of Magnetism and Magnetic Materials 321 (2009) 773–776

Contents lists available at ScienceDirect

Journal of Magnetism and Magnetic Materials

journal homepage: www.elsevier.com/locate/jmmm

Magnetic properties on shape memory alloys $Ni_2Mn_{1+x}In_{1-x}$

T. Kanomata [a,*], T. Yasuda [a], S. Sasaki [a], H. Nishihara [b], R. Kainuma [c], W. Ito [d], K. Oikawa [d], K. Ishida [d], K.-U. Neumann [e], K.R.A. Ziebeck [e]

[a] Faculty of Engineering, Tohoku Gakuin University, Tagajo 985-8537, Japan
[b] Faculty of Science and Technology, Ryukoku University, Otsu 520-2194, Japan
[c] Institute of Multidisciplinary Research for Advanced Materials, Tohoku University, Sendai 980-8577, Japan
[d] Department of Materials Science, Graduate School of Engineering, Tohoku University, Sendai 980-8579, Japan
[e] Department of Physics, Loughborough University, LE11 3TU, UK

ARTICLE INFO

Available online 3 December 2008

PACS:
75.30.Kz
81.30.Kf

Keywords:
Magnetic shape memory alloys
Martenstic transition
Phase diagram

ABSTRACT

X-ray powder diffraction and magnetization measurements were done on the magnetic shape memory alloys $Ni_2Mn_{1+x}In_{1-x}$. On the basis of the results, the magnetic phase diagram was determined for $Ni_2Mn_{1+x}In_{1-x}$ alloys. Magnetization measurements make clear that the excess Mn atoms, which substitute for In sites, are coupled ferromagnetically to the ferromagnetic manganese sublattices. A magnetic phase diagram of $Ni_2Mn_{1+x}In_{1-x}$ alloys is discussed qualitatively on the basis of the interatomic dependence of the exchange interactions.

1. Introduction

Ferromagnetic shape memory alloys (FSMAs) have attracted much attention due to their potential application as smart materials. They show a large magnetic-field-induced strain by the rearrangement of twin variants in the martensite phase [1]. Unlike the case of conventional shape memory alloys, the speed of the shape memory change is not limited in this mechanism. Thus, the FSMAs are potential materials for a magneto-mechanical actuator. Among them, the Ni–Mn–Ga alloys were mostly studied [2].

Recently, Sutou et al. [3] found that the Heusler alloys $Ni_{50}Mn_{50-x}Z_x$($Z=$ In, Sn and Sb) show the martensitic transition from the $L2_1$ structure to an orthorhombic four-layered one. The magnetization in the martensite phase for $Ni_{50}Mn_{50-x}Z_x$($Z=$ In, Sn and Sb) is much smaller compared to that in the austenite one.

More recently, the present author's group has found an unusual type of FSMAs showing the martensitic transition from the ferromagnetic austenite phase to the nonmagnetic martensite phase in Ni–Co–Mn–In Heusler alloys and confirmed the magnetic-field-induced reverse martensitic transition [4]. An almost perfect shape memory effect associated with this phase change is induced by a magnetic field and is called the metamagnetic shape memory effect. This alloy system opens up to the possibility of utilizing the magnetic-field-induced shape memory effect. Since then, the magnetic shape memory alloys Ni–Mn–Z ($Z=$ In, Sn and Sb) have attracted much attention from the point of view of high-performance materials being controlled by a magnetic field [5,6].

To understand the magnetic-field-induced shape memory effect in Ni–Mn–Z ($Z=$ In, Sn and Sb) alloys, we have investigated the magnetic and crystallographic properties of $Ni_2Mn_{1+x}In_{1-x}$ ($0\leqslant x\leqslant 0.60$) alloys.

2. Experimental

The polycrystalline $Ni_2Mn_{1+x}In_{1-x}$ ($0\leqslant x\leqslant 0.60$) alloys were prepared by the repeated melting of the appropriate quantities of the constituent elements, namely 99.99% pure Ni, 99.95% pure Mn and 99.99% pure In, in an argon arc furnace. Subsequently, samples were sealed in the evacuated double silica tubes, heated at 850 °C for 3 days and then quenched in water. The phase identification and characterization of the samples were carried out by X-ray powder diffraction using Cu-Kα radiation.

The magnetization measurements were made using a commercial superconducting quantum interference device (SQUID) magnetometer in fields up to 50 kOe.

3. Results

The crystal structure of the Heusler alloy Ni_2MnIn is shown in Fig. 1. The Heusler unit cell is comprised of four interpenetrating fcc lattices A, B, C and D. The Ni atoms occupy the corner (A and C) sites of the bcc structure, while the Mn and In atoms occupy

* Corresponding author. Tel.: +81 22 368 7249; fax: +81 22 368 7070.
E-mail address: kanomata@tjcc.tohoku-gakuin.ac.jp (T. Kanomata).

0304-8853/$ - see front matter
doi:10.1016/j.jmmm.2008.11.079

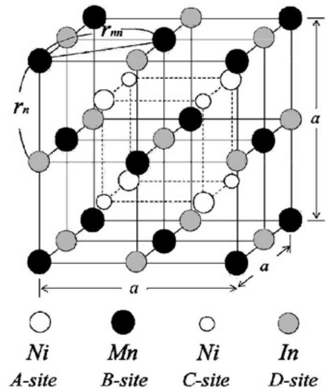

Fig. 1. Unit cell of the Heusler-type alloy Ni_2MnIn. The sites are presented by A, B, C and D. The A and C sites are equivalent and occupied by Ni atoms, the B site is occupied by Mn, and the D site by In. r_n represents the nearest Mn–In interatomic distance and r_{nn} the nearest Mn–Mn one on the Mn sites.

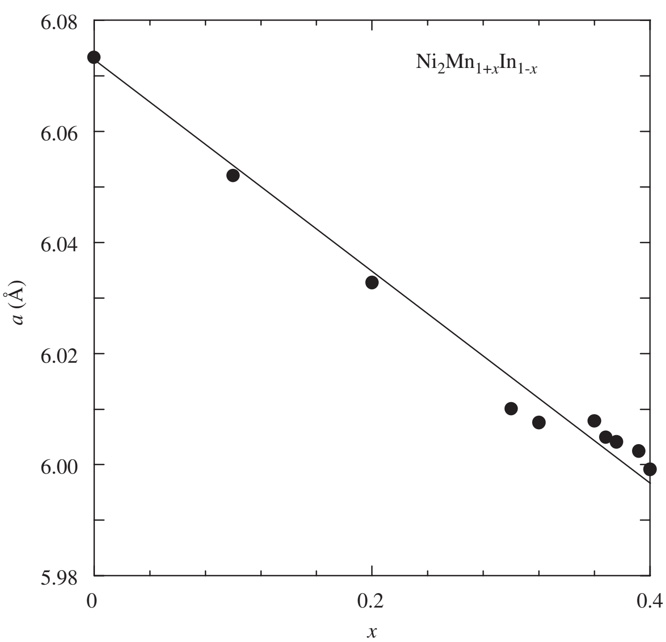

Fig. 2. Lattice parameter a versus concentration x curve for $Ni_2Mn_{1+x}In_{1-x}$ alloys at room temperature. Solid line in the figure is a guide for the eyes.

alternate body center (B and D, respectively) sites. For $Ni_2Mn_{1+x}In_{1-x}$ alloys, the samples with $x \leqslant 0.40$ are shown to crystallize in the $L2_1$ structure at room temperature by the X-ray powder diffraction measurements. Fig. 2 shows the concentration dependence of the lattice parameter a of $Ni_2Mn_{1+x}In_{1-x}$ alloys. The lattice parameter decreases linearly with the concentration x, which can be attributed to the difference in the ionic radii of the Mn and In atoms. The structural refinement of $Ni_2Mn_{1+x}In_{1-x}$ $(0 \leqslant x \leqslant 0.40)$ alloys was performed by X-ray powder diffraction data using the standard Rietveld technique. We confirmed that the excess Mn atoms on $Ni_2Mn_{1+x}In_{1-x}$ $(0< x \leqslant 0.40)$ alloys occupy the vacant In sites. Recently, Krenke et al. [7] investigated the crystal structure of the magnetic shape memory alloy $Ni_{1.988}Mn_{1.372}In_{0.640}$ in the martensite phase using the neutron powder diffraction measurements. According to the results, $Ni_{1.988}Mn_{1.372}In_{0.640}$ alloy crystallizes in the $L2_1$ structure in the austenite phase. At 5 K, the diffraction pattern is that of a 10 M modulated martensite structure having a monoclinic unit cell with $\beta = 86.97^\circ$ and lattice constants $a = 4.398$, $b = 5.635$ and

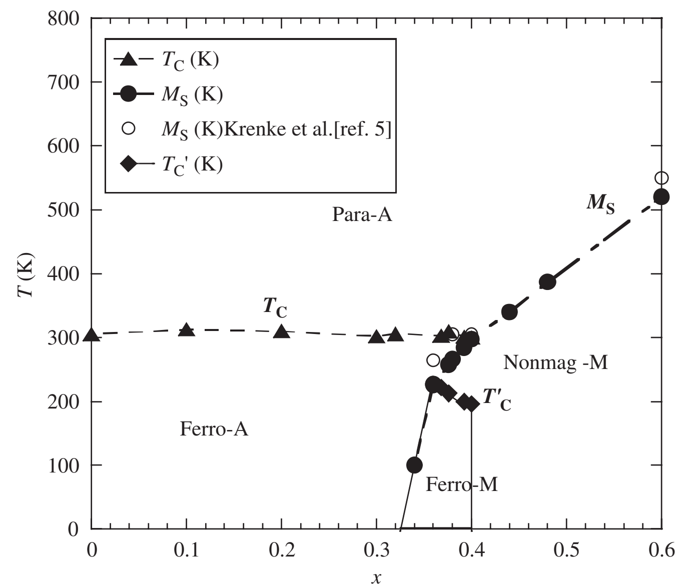

Fig. 3. Phase diagram of $Ni_2Mn_{1+x}In_{1-x}$ alloys, where Para, Ferro and Nonmag mean paramagnetic, ferromagnetic-like and nonmagnetic states, respectively, and A and M indicate the austenite and martensite phases, respectively. T_C and T'_C indicate the Curie temperature of the austenite phase and the martensite one, respectively. M_s means the martensitic start temperature.

$c = 21.720$ Å. Other than this slight monoclinicity, the structure is orthorhombic, having a shuttle periodicity of ten lattice planes in the [1 1 0] direction.

More recently, we have carried out precise magnetization and initial permeability measurements on $Ni_2Mn_{1+x}In_{1-x}$ $(0 \leqslant x \leqslant 0.60)$ alloys. Based on these experimental results, the phase diagram of $Ni_2Mn_{1+x}In_{1-x}$ $(0 \leqslant x \leqslant 0.60)$ alloys was determined as shown in Fig. 3. The phase diagram of $Ni_2Mn_{1+x}In_{1-x}$ alloys was reported first by Sutou et al. [3]. Then, Ito et al. [8] and Krenke et al. [5] revised the magnetic phase diagram for $Ni_2Mn_{1+x}In_{1-x}$ alloys. The phase diagram shown in Fig. 3 is in good agreement of their diagrams. Data from the literature are also included in Fig. 3. As seen in the figure, the Curie temperature T_C of the austenite phase shows very little change with x. The martensitic transition is observed for the samples with $0.32 \leqslant x \leqslant 0.60$ with the martensitic start temperature M_s increasing abruptly with x. The nonmagnetic (Nonmag-M) and the ferromagnetic-like (Ferro-M) states appear below M_s. On the other hand, the Curie temperature T'_C of the martensite phase decreases linearly with x. It is not possible to determine from the present data the exact magnetic structures of the Nonmag-M state and Ferro-M one at these temperatures. More recently, we have obtained the Mössbauer spectra of $Ni_2Mn_{1.48}Fe_{0.04}Sn_{0.48}$ alloy at various temperatures using ^{57}Fe as a probe. The spectra in the Nonmag-M state show a single peak, suggesting that the Nonmag-M is a paramagnetic state [9]. It should be noted that the phase diagram of $Ni_2Mn_{1+x}In_{1-x}$ alloys is very similar to that of $Ni_2Mn_{1+x}Sn_{1-x}$ alloys [10].

The magnetization curves at 5 K for $Ni_2Mn_{1+x}In_{1-x}$ alloys with various concentration x are shown in Fig. 4. The magnetization M at 5 K is saturated in a field of about 10 kOe. The spontaneous magnetization at 5 K for $Ni_2Mn_{1+x}In_{1-x}$ $(0 \leqslant x \leqslant 0.408)$ alloys was determined by the linear extrapolation to $H/M = 0$ of the M^2 versus H/M curves. The magnetic moment per formula unit at 5 K, μ^{tot}, for $Ni_2Mn_{1+x}In_{1-x}$ alloys was estimated from the spontaneous magnetization and is plotted against x as shown in Fig. 5. The values of the magnetic moment for the samples with $0.368 \leqslant x \leqslant 0.408$ are much smaller than those for the samples with $0 \leqslant x \leqslant 0.32$. Fig. 5 suggests that the magnetic coupling at 5 K